Tetrahedron 65 (2009) 6959–6964

Contents lists available at ScienceDirect

Tetrahedron

journal homepage: www.elsevier.com/locate/tet

A colorimetric and fluorescent turn-on chemosensor for Zn^{2+} based on an azobenzene-containing compound

Jing Wang, Chang-Sik Ha *

Department of Polymer Science and Engineering, Pusan National University, Busan 609-735, Republic of Korea

ARTICLE INFO

Article history:
Received 1 May 2009
Received in revised form 12 June 2009
Accepted 15 June 2009
Available online 18 June 2009

Keywords:
Chemosensor
Fluorescent
Colorimetric
Zinc ion
Azobenzene-containing

ABSTRACT

This paper presents a new colorimetric reversible fluorescent turn-on chemosensor molecule for zinc ion based on an azobenzene derivative. The basal fluorescence intensity of the chemosensor molecule is little affected under physiological pH 5–9, whilst the excitation (507 nm) and emission (610 nm) wavelength of the molecular probe for zinc ion is in the visible range.

1. Introduction

The design and synthesis of chemosensors with high selectivity and sensitivity for heavy and/or transition metal (HTM) ions continues to be an active area of supramolecular chemistry.[1–9] Since Zinc is the second-most-abundant transition-metal ion in the human body, the detection and imaging of Zn^{2+} in biological samples are of paramount interest owing to the role of this cation in physiological functions. As Zn^{2+} is invisible to most analytical techniques, fluorescence techniques stand out as the method of choice. This method utilizes a probe molecule that recognizes Zn^{2+} and emits a specific wavelength upon binding, which in turn allows tracking of zinc ions in live cells with fluorescence microscopy.[10–25] Metal coordination compounds with 2,2′-dihydroxyazoarenes are well known.[26,27] Studies on complexes involving 2,2′-dihydroxyazobenzene as ligand have been described.[28–39] However, derivatives of 2,2′-dihydroxyazobenzene suggested for sensing of metal ions is still rare.[40]

Herein, we present a new colorimetric fluorescent turn-on chemosensor molecule that responds to zinc ion using an azobenzene-containing fluorescent molecule, compound **1** (see Scheme 1). There are several advantages for this new fluorescent Zn^{2+} chemosensor molecule. First, **1** has no emission signal at 610 nm in the absence of Zn^{2+}, and the emission signal at 610 nm and large Stokes shift of 103 nm appear in the presence of Zn^{2+}. Second, the colour change from light yellow (in the absence of Zn^{2+}) to reddish orange (in the presence of Zn^{2+}) can be distinguished easily by the naked eye, while subsequent addition of ethylenediamine tetraacetic acid (EDTA) results in recovery of the original colour. Third, the chemosensor molecule is selective for Zn^{2+} without interference other biologically important metal ions, such as Cu^{2+} and Mg^{2+}. Fourth, the excitation and emission wavelength of the molecular probe is in the visible range that can minimize cell and tissue damage. This observation indicates that the molecular probe may be useful for sensing and imaging of zinc ions under physiological conditions.

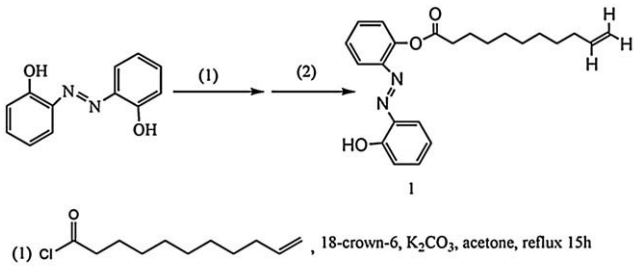

(2) Column chromatography, eluent ratio of petroleum ether and ethyl acetate is from 10/1 to 5/1.

Scheme 1. Synthetic route to the fluorescent chemosensor molecule, compound **1**.

* Corresponding author. Tel.: +82 51 510 2407; fax: +82 51 514 4331.
E-mail address: csha@pusan.ac.kr (C.-S. Ha).

0040-4020/$ – see front matter © 2009 Elsevier Ltd. All rights reserved.
doi:10.1016/j.tet.2009.06.055

2. Results and discussion

2.1. Synthesis and characterization

1 was derived from 2,2-dihydroxyazobenzene (DHAB) and 10-undecenoyl chloride, and was characterized by Fourier-transform infrared (FTIR) spectroscopy, ^{1}H nuclear magnetic resonance (NMR) spectroscopy, thin layer chromatography (TLC) and electrospray ionization mass-spectrometry (ESI-MS). The synthesis of compound **1** is straightforward and is illustrated in Scheme 1.

1 has two tautomeric forms, the azo form and hydrazone form (see Fig. 1). Intramolecular hydrogen bonds[41] are present irrespective of the form that it takes. The FTIR spectra showed a weak narrow band at 3072 cm^{-1}, indicating the absence of free OH and NH groups due to the formation of stable intramolecular hydrogen bonds. The band at 3072 cm^{-1} was assigned to the vibration of a N–H group, which participates in the intramolecular hydrogen bond, NH···O (see Supplementary data, Fig. S1).

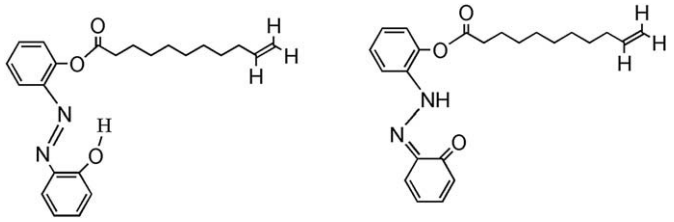

Figure 1. Two tautomeric forms (azo form (left) and hydrazone form (right)) of **1**.

2.2. Effect of pH

The deprotonation and protonation behaviour of **1** at various pH values were examined (Scheme 2). A strong base, sodium hydroxide, was used to deprotonate **1**. A change in the UV–vis spectra and fluorescence intensity was observed while the colour of the solution changed from light yellow to reddish orange (see Figs. 2–4 and Supplementary data, Fig. S2). As indicated in Figure 3, the bands at approximately 325 nm and 477 nm were assigned to the π–π* transition of the azo form and the band at approximately 384 nm was assigned to the π–π* transition of the hydrazone form.[41] Clearly, the π–π* band of **1** at approximately 325 nm decreased and that at 384 nm disappeared, while a new peak appeared at 477 nm with increasing pH, i.e., **1** exists as the azo form alone. The red-shift in absorption encountered after adding a base is consistent with the deprotonation of the hydroxyl group (pK_a=9.38, see Fig. S3) in the neutral form to yield an anionic species. This results in an increase in the electron density of Ph–N=N–Ph, which leads to an increase in electron delocalization (Scheme 2). This delocalized π-conjugated bond is energetically higher, resulting in a red shift in the π–π* transition from 325 nm to 477 nm and a significantly higher fluorescence intensity. Importantly, this process can be reversed completely by adding acid (hydrochloric acid), thereby recovering the absorption and FL spectra. The protonation of **1** was also examined (see Scheme 2) using a strong acid, hydrochloric acid. When H^+ approaches **1**, it should attack the electron-rich nitrogen atom,[42] but the absorption and FL spectra changed slightly (see Figs. 3 and 4 and Supplementary data, Fig. S2). The results suggest that the basal fluorescence intensity of **1** is little affected under physiological pH 5–9. It should be noteworthy that this aspect is quite important for many further biological applications that the sensor molecule doesn't respond to changes in pH.

2.3. Selectivity to metal ions

The metal selectivity of **1** is illustrated in Figure 5, Figures S4 and S5. Upon adding alkali and alkaline earth metal ions such as K^+ and Mg^{2+}, the absorption spectra changes slightly. After addition of transition metal ions except for Fe^{3+}, the typical absorption peak for **1** at 325 nm decreases, while a new absorption peak at around 500 nm appeared due to the formation of complex between **1** and metal ions. In order to further study the selectivity of **1** toward metal ions, fluorescence spectra were measured using two excitation wavelengths (320 nm and 507 nm) based on the two absorption peaks. For λ_{ex}=320 nm, alkali and alkaline earth metal ions such as K^+ and Mg^{2+} do not result in any significant response from **1**. However, transition metal ions increase or quench the fluorescence intensity at 355 nm slightly. Surprisingly, a new peak at around 600 nm appeared only after adding Zn^{2+}. With λ_{ex}=507 nm, **1** displayed a large CHEF (chelation-enhanced fluorescence) effect only with Zn^{2+}, whereas minimal or no changes were observed with the other metal ions. When Mg^{2+}, Cu^{2+}, Co^{2+} or Cd^{2+} were added to the **1**/Zn^{2+} system, the fluorescence intensity was little affected, meaning that the sensing of **1** for Zn^{2+} was not influenced by other metal ions. Thus, it may be concluded that **1** has special selectivity and sensitivity to Zn^{2+}.

2.4. Detection of Zn^{2+}

At neutral state, upon coordinating Zn^{2+}, the deprotonation of **1** is promoted,[10] the elevated electron density after Zn^{2+}-coordination decreases the energy gap between HOMO and LUMO of the π–π* transition, and the absorption spectra undergoes a red-shift, the typical absorption peak for the hydrazone form of **1** disappeared, and the colour of the solution changed from light yellow to reddish orange (Figs. 6–8 and Fig. S6). For λ_{ex}=507 nm, free **1** (Φ_F=0.0029) has little detectable fluorescence at 610 nm, a distinct enhancement of the fluorescence intensity at 610 nm (Φ_F=0.17) and large stokes shift of 103 nm was observed upon interaction with

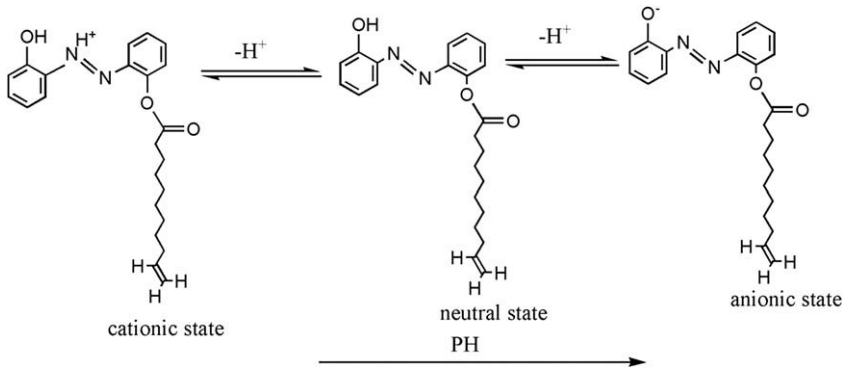

Scheme 2. Deprotonation and protonation behavior of **1**.

Figure 2. Images of **1** at different pH in a mixture of H_2O/MeOH (4:6, v/v, with 10.0 mM buffer), the number on each bottle represents the pH of the solution.

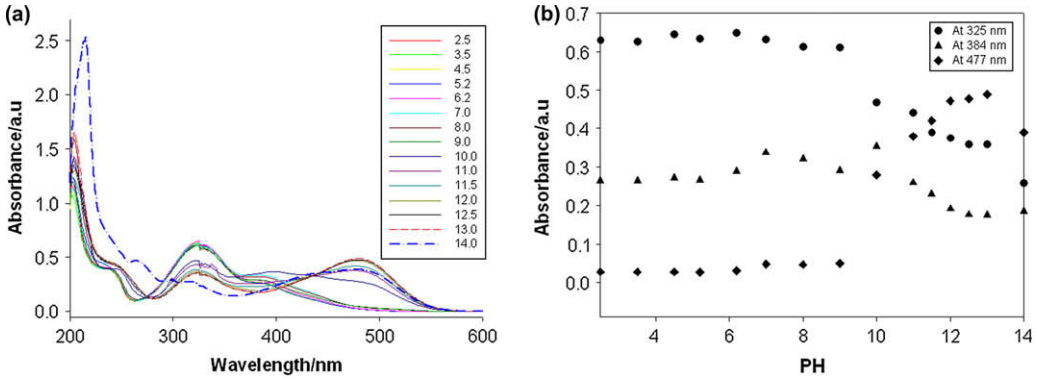

Figure 3. (a) Change in the UV–vis absorption spectra of **1** (6×10^{-5} M) in a mixture of H_2O/MeOH (4:6, v/v, with 10.0 mM buffer) at different pH; (b) effect of pH on the change in the absorption spectra of **1** (6×10^{-5} M) in a mixture of H_2O/MeOH (4:6, v/v, with 10.0 mM buffer) at 325 nm, 384 nm and 477 nm.

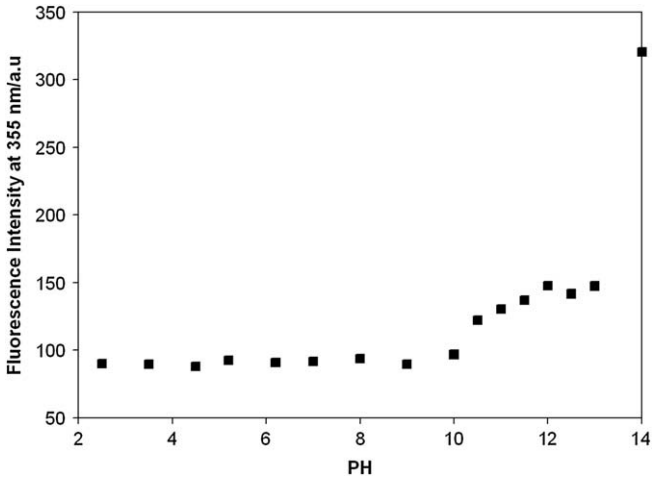

Figure 4. Effect of pH on the changes in fluorescence intensity of **1** (6×10^{-5} M) in a mixture of H_2O/MeOH (4:6, v/v, with 10.0 mM buffer).

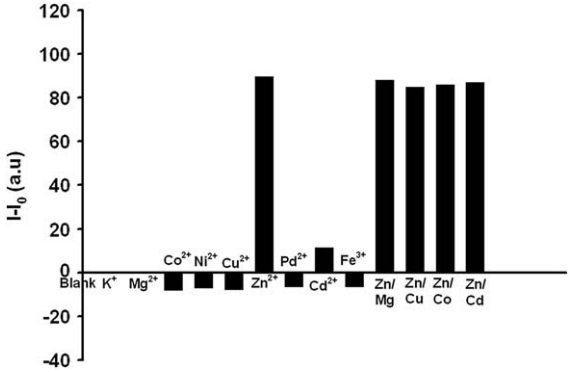

Figure 5. Fluorescence intensity changes of **1** (3×10^{-5} M) in a mixture of H_2O/MeOH (4:6, v/v, 10 mM HEPES at pH 7.0) in the presence of various metal ions (1.5×10^{-4} M), λ_{ex}=507 nm. Metal ions from left to right: blank, K^+, Mg^{2+}, Co^{2+}, Ni^{2+}, Cu^{2+}, Zn^{2+}, Pd^{2+}, Cd^{2+}, Fe^{3+}, Zn^{2+} and Mg^{2+}, Zn^{2+} and Cu^{2+}, Zn^{2+} and Co^{2+}, Zn^{2+} and Cd^{2+}. I and I_0 are the fluorescence intensity of **1** in the presence and absence of various metal ions.

5 equiv Zn^{2+} (Fig. 6a and Fig. S7). An enhancement factor (EF, I/I_0) of above 15 at 610 nm was found in the presence of 5 equiv of Zn^{2+} which was attributed to the formation of the complex between **1** and Zn^{2+} (Fig. 6a). A peak at m/z 825.2 in the electrospray ionization (ESI) HPLC mass spectra (Fig. S8) provides strong evidence for the formation of the complex for **2**(**1**)–Zn^{2+}.[43a] The approximate Job's plot[43] also suggests that **1** forms a 2:1 complex with Zn^{2+} (Fig. 6b), with a K_{ass} of 4.0×10^5 M^{-2}, as calculated from non linear least-square equation (see Supplementary data, Eq. 1[6,44]). In addition, we confirmed the reversibility of the fluorescence intensity and color change of **1** by removing the Zn^{2+} ion bound to **1** by treatment with a strong chelate ethylenediamine tetraacetic acid (EDTA) due to the great difference in association constant (K_{ass}) between EDTA and **1** with Zn^{2+} ions (log K_{ass} of EDTA with Zn^{2+} is 16.4, which indicates that EDTA binds much more strongly with Zn^{2+} ion than **1**[45]) (see Fig. 8). As expected, the reddish orange color of **1** in the presence of Zn^{2+} ion was changed into the original light yellow upon the EDTA treatment. Because Zn^{2+} ion bound to **1** is dissociated by EDTA, **1** can be repeatedly used by renewing with EDTA. Moreover, the absorption spectra and the fluorescence intensities of **1** in the presence of 5 equiv of Zn^{2+} ion at pH values ranging from 4.0 to 12.0 were measured (see Supplementary data, Figs. S9–S11). As expected, **1**–Zn(II) complex is not subject to interference induced by pH changes and exhibits almost constant fluorescence intensity at pH values above 5.0.

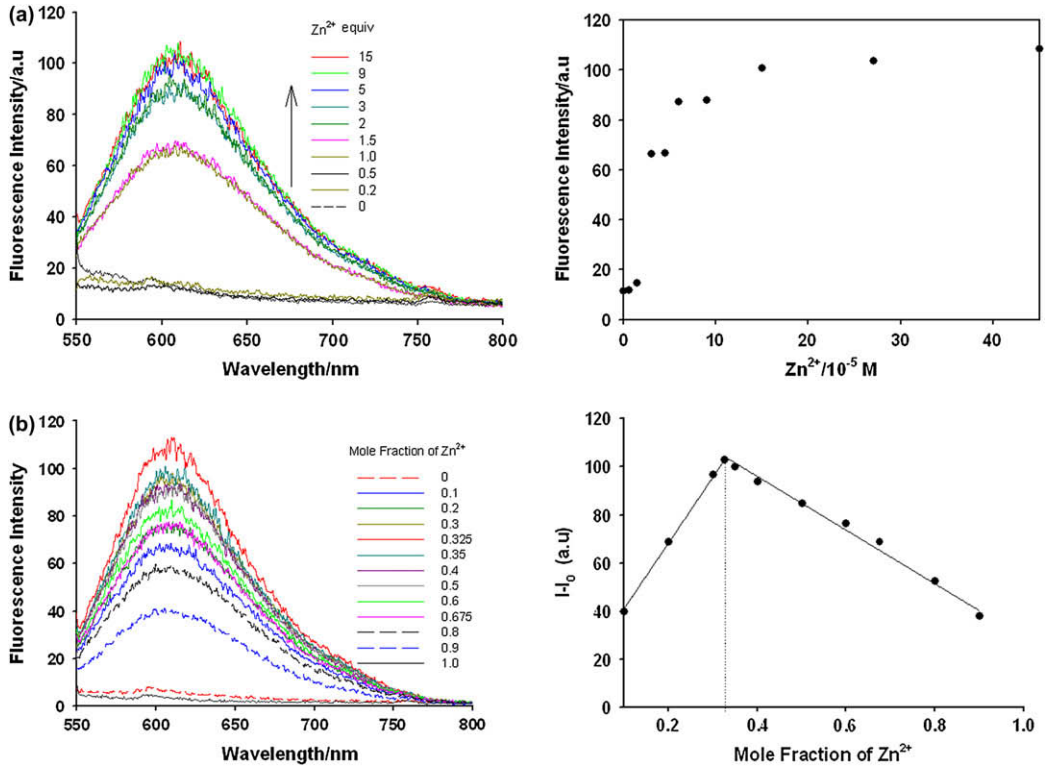

Figure 6. (a) Fluorescence emission spectra of **1** upon progressive addition of Zn^{2+} and fluorescence intensity at 610 nm versus concentration of Zn^{2+} ions (3×10^{-5} M) in a mixture of H_2O/MeOH (4:6, v/v, 10 mM HEPES at pH 7.0), λ_{ex}=507 nm. The arrow indicates the spectral change upon addition of Zn^{2+}; (b) Job's plots of **1** and Zn^{2+}, λ_{ex}=507 nm, λ_{em}=610 nm; I and I_0 are the fluorescence intensity of **1** in the presence and absence of Zn^{2+}, respectively; the total concentration of **1** and Zn^{2+} ion is 0.1 mM, pH 7.0.

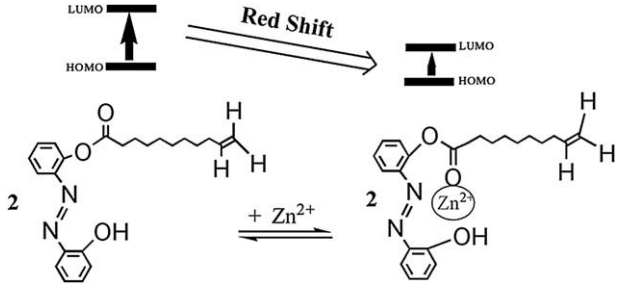

Figure 7. Metal ion-coordination-promoted deprotonation causes the bathochromic shift of the spectra of **1**.

3. Conclusions

In conclusion, we report a new colorimetric reversible fluorescent turn-on chemosensor molecule for zinc ion. The long-visible-wavelength excitation (507 nm) and emission (around 600 nm) profile of the molecular probe minimizes cell and tissue damage. The remarkable difference in the emission color of the molecular probe before and after Zn^{2+} binding is of advantage for imaging applications. A 'turn-on' emission or shift in the emission color upon binding to Zn^{2+} should be ideal for in vivo imaging. This observation indicates that the probe may be useful for sensing and imaging of zinc ions under physiological conditions. It is likely that the observations made in this effort will provide the basis for a new strategy for the design of azobenzene based fluorescent chemosensor molecules. The insensitivity of **1**–Zn(II) complex to pH opens the way to the design of fluorosensor molecules for anions, whose recognition processes are based on the metal–ligand interaction. We are currently working along these lines.

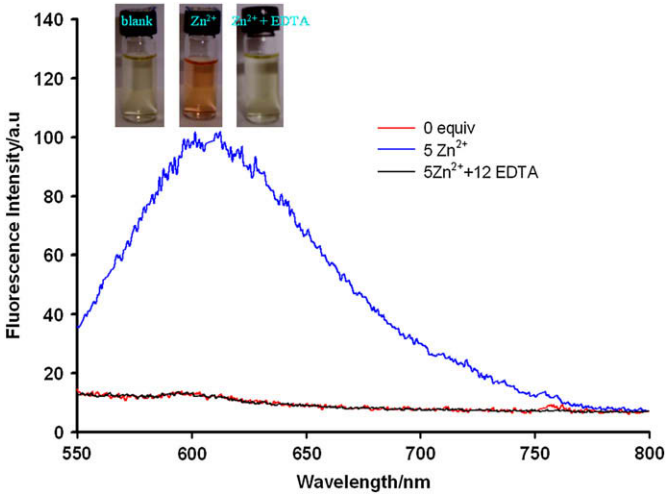

Figure 8. Fluorescence emission spectra of **1** (3×10^{-5} M) in a mixture of H_2O/MeOH (4:6, v/v, 10 mM HEPES at pH 7.0), λ_{ex}=507 nm and visual color changes of **1** in a mixture of H_2O/MeOH (4:6, v/v, 10 mM HEPES at pH 7.0) upon addition of 5 equiv Zn^{2+} and 12 equiv EDTA.

4. Experimental

4.1. General

Thin layer chromatography (TLC) was carried out on alumina backed plates coated with Merck silica gel F_{254}. Column chromatography was performed on silica gel 60F (Merck 9385, 0.040–0.063 nm). The Fourier-Transform Infrared (FTIR) spectra were recorded at room temperature on a JASCO FTIR 460 Plus operated at a resolution 4 cm^{-1}. ^1H NMR spectra were recorded on a Varian

Gemimi-2000 (300 MHz) spectrometer. Electrospray Ionization (ESI) Mass-Spectrometry was performed using agilent 1100 LC/MSD SL instrument. The UV–vis spectra were measured using a Hitachi U-2010 spectrometer. The fluorescence emission spectra were measured using a Hitachi F-4500 spectrometer. Stock buffer solutions (20 mM) of various pH values were prepared in a MeOH/H_2O cosolvent (v/v, 6/4). PHP (potassium hydrogen phthalate, pH 2.5–5.0), MES (2-morpholineoethanesulfonic acid, pH 5.5–6.5), HEPES (4-(2-hydroxyethyl)piperazine-1-ethanesulfonic acid, pH 7.0–8.0), EPPS (4-(2-hydroxyethyl)piperazine-1-propanesulfonic acid, pH 8.2–8.5), and CHES (2-(cyclohexylamino)-1-ethanesulfonic acid, 9.0–10.0) were used to cover different pH ranges. pH above 10 was obtained by adding small amount of NaOH. 0.06 mM of **1** and 10.0 mM of buffer were used for both absorption and fluorescence measurements.

4.2. pK_a determination

The pK_a values were determined spectrophotometrically.[46] The spectra were observed from 200 nm to 600 nm initially and after each subsequent pH adjustment. The pH adjustments and spectroscopic measurements were made until an end-point was reached, and the pK_a values were obtained using the following equation:

$$\mathrm{p}K_a = \mathrm{pH} + \log_{10}\left(\frac{A - A_{\mathrm{In}^-}}{A_{\mathrm{HIn}} - A}\right)$$

where A is the absorbance, In^- and HIn are the deprotonated form (at 477 nm) and the protonated form (at 325 nm) of the compound, respectively. The reliability of an individual pK_a value was determined graphically and repeated twice for confirmation.

4.3. Quantum yield measurements

Quantum yields for fluorescence were measured by comparing the integrated area of the corrected emission spectrum of the samples with that of a solution of fluorescein in 0.1 N NaOH, which has a quantum efficiency of 0.95.[14,47] The quantum efficiency of the metal-free **1** was measured by using a dilute sample of **1** (1×10^{-6} M) in 10 mM HEPES, pH=7.0. The quantum efficiency of metal-bound compound was measured by using a dilute sample of **1** (8×10^{-7} M) and 5 equiv $ZnCl_2$ in 10 mM HEPES, pH=7.0. The concentration of the reference was adjusted to match the absorbance of the test sample at the wavelength of excitation. Emission for **1** and **1**–Zn^{2+} was integrated from 550 to 650 nm with excitation at 507 nm. The quantum yields were calculated with the following equation:

$$\Phi_F(\mathrm{x}) = \left(\frac{A_s}{A_x}\right)\left(\frac{F_x}{F_s}\right)\left(\frac{\eta_x}{\eta_s}\right)^2 \Phi_F(\mathrm{s})$$

where s is the standard, x is the unknown, A is the absorbance at the excitation wavelength, F is the integrated area under the emission curve, η is the refractive index of the solvent and Φ_F is the quantum yield.

4.4. Synthesis of compound 1

10-Undecenoyl chloride (2.3 mmol, 466 mg) was added to a mixture of 2,2′-dihydroxyazobenzene[35,48] (1.5 mmol, 321 mg), K_2CO_3 (4.5 mmol, 621 mg) and 18-crown-6 (50 mg) in dry acetone (50 ml) and the mixture was refluxed for 15 h. After cooling to room temperature, the mixture was filtered and evaporated. The residue was dissolved in ethyl acetate, washed with water and dried over $MgSO_4$. The resulting residue was then dried. The crude product was purified by column chromatography and eluted with a solvent gradient ranging from 10 to 20% ethyl acetate in petroleum ether to yield **1** as an orange solid (425 mg, 75% yield). ^{1}H NMR (300 MHz, $CDCl_3$, 25 °C, TMS): δ=7.01–7.94 (m, 8H), 5.81 (m, 1H), 4.95(t, 2H), 2.69 (m, 2H), 2.05 (m, 2H), 1.79 (m, 2H), 1.29–1.33 (m, 10H). MS-ESI (m/z): $[M+1]^+$ 381.3.

Acknowledgements

This work was supported by the Korea Science and Engineering Foundation (KOSEF) Grant funded by the Ministry of Education, Science and Technology, Korea (MEST) (Acceleration Research Program (No. 2009-0078791)), a grant from the Fundamental R&D program for Core Technology of Materials funded by the Ministry of Knowledge Economy, Korea, the Korea-China Joint Research Center Program of the Korea Foundation of International Cooperation for Science and Technology, the Brain Korea 21 Project, and the MEST for the scholarship for foreign students (J.W.).

Supplementary data

Supplementary data associated with this article can be found in the online version, at doi:10.1016/j.tet.2009.06.055.

References and notes

1. de Silva, A. P.; Gunaratne, H. Q. N.; Gunnlaugsson, T.; Huxley, A. J. M.; McCoy, C. P.; Rademacher, J. T.; Rice, T. E. *Chem. Rev.* **1997**, *97*, 1515.
2. Schmittel, M.; Lin, H. W. *Angew. Chem.* **2007**, *119*, 911.
3. Prodi, L.; Bolletta, F.; Montalti, M.; Zaccheroni, N. *Coord. Chem. Rev.* **2000**, *205*, 59.
4. Callan, J. F.; de Silva, A. P.; Magri, D. C. *Tetrahedron* **2005**, *61*, 8551.
5. Valeur, B. *Molecular Fluorescence Principles and Applications*; Wiley-VCH: Weinheim, 2002.
6. Guo, Z. Q.; Zhu, W. H.; Shen, L. J.; Tian, H. *Angew. Chem., Int. Ed.* **2007**, *46*, 5549.
7. Komatsu, K.; Kikuchi, K.; Kojima, H.; Urano, Y.; Nagano, T. *J. Am. Chem. Soc.* **2005**, *127*, 10197.
8. (a) Wang, H. H.; Gan, Q.; Wang, X. J.; Xue, L.; Liu, S. H.; Jiang, H. *Org. Lett.* **2007**, *9*, 4995; (b) Carol, P.; Sreejith, S.; Ajayaghosh, A. *Chem. Asian J.* **2007**, *2*, 338.
9. (a) Szaciłowski, K. *Chem. Rev.* **2008**, *108*, 3481; (b) Montenegro, J. M.; Perez-Inestrosa, E.; Collado, D.; Vida, Y.; Suau, R. *Org. Lett.* **2004**, *6*, 2353; (c) Kay, E. R.; Leigh, D. A.; Zerbetto, F. *Angew. Chem., Int. Ed.* **2007**, *46*, 72; (d) Tian, H.; Wang, Q. C. *Chem. Soc. Rev.* **2006**, *35*, 361.
10. Zhang, L.; Dong, S.; Zhu, L. *Chem. Commun.* **2007**, 1891.
11. Xu, Z. C.; Kim, G. H.; Han, S. J.; Jou, M. J.; Lee, C.; Shin, I.; Yoon, J. *Tetrahedron* **2009**, *65*, 2307.
12. (a) Hirano, T.; Kikuchi, K.; Urano, Y.; Higuchi, T.; Nagano, T. *Angew. Chem., Int. Ed.* **2000**, *39*, 1052; (b) Gee, R. K.; Zhou, Z. L.; Qian, W. J.; Kennedy, R. *J. Am. Chem. Soc.* **2002**, *124*, 776.
13. Nolan, E. M.; Lippard, S. J. *Acc. Chem. Res.* **2009**, *42*, 193.
14. Burdette, S. C.; Walkup, G. K.; Spingler, B.; Tsien, R. Y.; Lippard, S. J. *J. Am. Chem. Soc.* **2001**, *123*, 7831.
15. Aoki, S.; Kaido, S.; Fujioka, H.; Kimura, E. *Inorg. Chem.* **2003**, *42*, 1023.
16. Kiyose, K.; Kojima, H.; Urano, Y.; Nagano, T. *J. Am. Chem. Soc.* **2006**, *128*, 6548.
17. Zhang, L.; Clark, R. J.; Zhu, L. *Chem.—Eur. J.* **2008**, *14*, 2894.
18. Maruyama, S.; Kikuchi, K.; Hirano, T.; Urano, Y.; Nagano, T. *J. Am. Chem. Soc.* **2002**, *124*, 10650.
19. Kikuchi, K.; Komatsu1, K.; Nagano, T. *Curr. Opin. Chem. Biol.* **2004**, *8*, 182.
20. Walkup, G. K.; Burdette, S. C.; Lippard, S. J.; Tsien, R. Y. *J. Am. Chem. Soc.* **2000**, *122*, 5644.
21. Parkesh, R.; Lee, T. C.; Gunnlaugsson, T. *Org. Biomol. Chem.* **2007**, *5*, 310.
22. Liu, Y.; Zhang, N.; Chen, Y.; Wang, L. H. *Org. Lett.* **2007**, *9*, 315.
23. Wang, J. B.; Xiao, Y.; Zhang, Z. C.; Qian, X. H.; Yanga, Y. Y.; Xu, Q. *J. Mater. Chem.* **2005**, *15*, 2836.
24. Fabbrizzi, L.; Licchelli, M.; Mancin, F.; Pizzeghello, M.; Rabaioli, G.; Taglietti, A.; Tecilla, P.; Tonellato, U. *Chem.—Eur. J.* **2002**, *8*, 94.
25. Burdette, S. C.; Frederickson, C. J.; Bu, W. M.; Lippard, S. J. *J. Am. Chem. Soc.* **2003**, *125*, 1778.
26. Price, R. In *Comprehensive Coordination Chemistry*; Wilkinson, G., Gillard, R. D., McCleverty, J. A., Eds.; Pergamon: Oxford, 1987; Vol. 6, p 35.
27. Grychtol, K.; Mennike, W. *Ullmann's Encyclopedia of Industrial Chemistry*; Chemie: Weinheim, 1990; Vol. A16, p 299.
28. Abildgaard, J.; Hansen, P. E.; Josephsen, J.; Lycka, A. *Inorg. Chem.* **1994**, *33*, 5271.
29. Nag, J. K.; Chattopadhyay, P.; Mishra, T. K.; Sinha, C. *J. Indian Chem. Soc.* **2000**, *77*, 270.
30. Dutta, S.; Basu, P.; Chakravorty, A. *Inorg. Chem.* **1991**, *30*, 4031.
31. Chakravarty, J.; Dutta, S.; Chakravorty, A. *J. Chem. Soc., Dalton Trans.* **1993**, 2857.
32. Chakravarty, J.; Dutta, S.; Chandra, S. K.; Basu, P.; Chakravorty, A. *Inorg. Chem.* **1993**, *32*, 4249.

33. Dutta, S.; Basu, P.; Chakravorty, A. *Inorg. Chem.* **1993**, *32*, 5543.
34. Hintermaier, F.; Kuehlwein, F.; Robl, C.; Beck, W. *Z. Anorg. Allg. Chem.* **1995**, *621*, 829.
35. Adams, H.; Bucknall, R. M.; Fenton, D. E.; Garcia, M.; Oakes, J. *Polyhedron* **1998**, *17*, 4169.
36. Besslera, K. E.; Santosa, J. A.; Deflona, V. M.; Lemosa, S. S.; Niquet, E. *Z. Anorg. Allg. Chem.* **2004**, *630*, 742.
37. Lahiri, G. K.; Bhattacharya, S.; Mukherjee, M.; Mukherjee, A. K.; Chakravorty, A. *Inorg. Chem.* **1987**, *26*, 3359.
38. Cuny, G. D.; Landgrebe, K. D.; Smith, T. P. *Bioorg. Med. Chem. Lett.* **1999**, *9*, 237.
39. Iki, N.; Hoshino, H.; Yotsuyanagi, T. *Anal. Chem.* **2000**, *72*, 4812.
40. Yamamoto, K.; Sunada, H.; Yonezawa, Y.; Otsuka, A. *Bunseki Kagaku* **1991**, *40*, 495.
41. Bershtein, I. Y.; Ginzburg, O. F. *Russ. Chem. Rev.* **1972**, *41*, 97.
42. (a) Men, Y.; Korupoju, S. R.; Kurihara, M.; Mizutani, J.; Nishihara, H. *Chem.—Eur. J.* **2005**, *11*, 7322; (b) Kuwabara, T.; Shiba, K.; Nakajima, H.; Ozawa, M.; Miyajima, N.; Hosoda, M.; Kuramoto, N.; Suzuki, Y. *J. Phys. Chem. A* **2006**, *110*, 13521.
43. (a) Lee, H. Y.; Bae, D. R.; Park, J. C.; Song, H.; Han, W. S.; Jung, J. H. *Angew. Chem., Int. Ed.* **2009**, *48*, 1239–1243; (b) Huang, X. M.; Guo, Z. Q.; Zhu, W. H.; Xie, Y. S.; Tian, H. *Chem. Commun.* **2008**, 5143; (c) Tang, B.; Huang, H.; Xu, K. H.; Tong, L. L.; Yang, G. W.; Liu, X.; An, L. G. *Chem. Commun.* **2006**, 3609.
44. Zeng, L.; Miller, E. W.; Pralle, A.; Isacoff, E. Y.; Chang, C. J. *J. Am. Chem. Soc.* **2006**, *128*, 10.
45. Zhang, D.; Zhang, Q.; Su, J. H.; Tian, H. *Chem. Commun.* **2009**, 1700.
46. Sun, K. M.; McLaughlin, C. K.; Lantero, D. R.; Manderville, R. A. *J. Am. Chem. Soc.* **2007**, *129*, 1894.
47. Brannon, J. H.; Magde, D. *J. Phys. Chem.* **1978**, *82*, 705.
48. Lee, K.; Jang, B. B.; Kwon, W. J.; Suh, J. *J. Polym. Sci.: Part A: Polym. Chem* **1999**, *37*, 4117.